Propagation and termination processes in free-radical copolymerization of styrene and ethyl acrylate

Yung-Dae Ma* and Pan-Soo Kim†
Department of Polymer Science and Engineering, Dankook University, San 8, Hannam-dong, Yongsan-ku, Seoul 140, Korea

and Keiji Kubo‡ and Takeshi Fukuda*
Institute for Chemical Research, Kyoto University, Uji, Kyoto 611, Japan
(Received 2 August 1993; revised 8 September 1993)

The propagation and termination processes in free-radical copolymerization of styrene (**1**) and ethyl acrylate (**2**) in the bulk at 40°C were examined by the rotating-sector technique. A marked penultimate-unit effect was observed for the terminal radical **1** ($s_1 = 0.27$), in conformity with the prediction of the stabilization energy model. The concentration of the terminal radical **2** in this system was too small for the details about this radical to be elucidated. The termination process conforms to the notion of diffusion control, but conclusively not to that of chemical control. The experimental data, however, were not described very accurately by the North diffusion model. An alternative simple, no-parameter model, conceptually analogous to the Ito–O'Driscoll model, was proposed and found to describe the experiments better.

(Keywords: radical copolymerization; rate constants; penultimate effect)

INTRODUCTION

In recent years, the propagation and termination processes in free-radical copolymerization have been studied by various methods, such as spatially intermittent polymerization (s.i.p.)[1], rotating sector (r.s.)[2–4], pulsed laser polymerization (p.l.p.)[5–9] and electron spin resonance (e.s.r.)[10] techniques. As a result, fundamental defects of the classical copolymerization theory based on the terminal model (Mayo–Lewis model) have been disclosed. Namely, it has been observed in many systems that while the terminal model describes the composition curves well, it fails to predict the absolute values of propagation rate constant and polymerization rate.

Such failure of the classical model was originally reported for the bulk copolymerization of styrene (ST; **1**) and methyl methacrylate (MMA; **2**)[2]. A subsequent study on the solution copolymerization of ST and MMA has shown that the failure should be ascribed to a penultimate-unit effect (p.u.e.) and not to reaction environment effects[4]. In an attempt to explain the experimental results, we have proposed that radical stabilization energies are influenced by penultimate units. This postulate, along with the Evans–Polanyi-type argument, has led to the prediction[11–13] that:

$$s_1 s_2 = r_1 r_2 \tag{1}$$

where $s_1 = k_{211}/k_{111}$ and $s_2 = k_{122}/k_{222}$; k_{ijm} is the rate constant for the reaction of radical $\sim\sim\sim\sim\sim M_i M_j^*$ with monomer M_m ($i, j, m = \mathbf{1}$ or **2**). According to this 'stabilization energy model', the monomer reactivity ratios r_1 and r_2 do not depend on composition, as many experiments demand, but their absolute values are governed by p.u.e. This type of p.u.e. has been termed the 'implicit' p.u.e. to distinguish it from the 'explicit' p.u.e. that appears in composition (or sequence distribution) as well as in propagation rate. Experiments suggest that the implicit p.u.e. is a very general phenomenon, and that the correlation of $s_1 s_2$ and $r_1 r_2$ may be real. However, more experimental data of high quality are needed to reach a fundamental understanding of the copolymerization mechanism and the nature of p.u.e.

In this paper, we present a nearly complete set of experimental data for the bulk copolymerization of ST and ethyl acrylate (EA) at 40°C, carefully collected by the r.s. method. There are two main purposes in this work. The first is to make a contribution towards a better understanding of the propagation process and in particular to test equation (1). Two systems (ST/methyl acrylate (MA) and ST/butyl acrylate (BA)) akin to ST/EA have already been studied by the p.l.p. technique[8]. One would expect the kinetic behaviour of the ST/EA system to be similar to those systems. It turned out, however, that this is not necessarily the case (see below).

The second purpose of this work concerns the termination process. The termination rate constants in ST/alkyl acrylate systems have not been measured to date. Previous studies have shown that the termination step in radical copolymerization is controlled by diffusion, not by chemistry[1–4,7,10]. However, further details remain

* To whom correspondence should be addressed
† Present address: Institute of Polymer Engineering, University of Akron, Akron, OH 44325, USA
‡ Present address: Kuraray Co., Ltd, Kurashiki, Okayama 715, Japan

0032-3861/94/07/1375–07

unclear. The ST/EA system is particularly interesting because the termination rate constants for pure ST and EA are very different from each other, which offers an advantage in model discrimination. A brief preliminary account of this work has been given elsewhere[12–14].

EXPERIMENTAL

Materials

Commercial products of ST, EA, 2,2′-azobis(isobutyronitrile) (AIBN), 2,2′-azobis-(cyclohexane-1-carbonitrile) (ACN) and 4-hydroxy-2,2,6,6-tetramethylpiperidinyl-1-oxy (HTMPO) were purified as described elsewhere[2].

Volume contraction factor

The volume contraction factor, Γ°, for incipient copolymerization in the bulk was evaluated on the basis of the previously proposed equation[2,15,16]:

$$\Gamma^\circ = (F_1\Gamma_1^\circ + F_2\Gamma_2^\circ)(1 - a_{12}x_1x_2) - F_{12}\Delta V_{12} + x_2F_1(a_{12}V_1 + \tilde{V}_{1,1}^\circ - \tilde{V}_{1,2}^\circ) + x_1F_2(a_{12}V_2 + \tilde{V}_{2,2}^\circ - \tilde{V}_{2,1}^\circ) \quad (2)$$

$$\Gamma_1^\circ = V_1 - \tilde{V}_{1,1}^\circ, \qquad \Gamma_2^\circ = V_2 - \tilde{V}_{2,2}^\circ \quad (3)$$

The symbols in equations (2) and (3) have the same meaning as those in the previous paper[2]. For example, $x_1 = 1 - x_2$ represents the volume fraction of monomer **1** before mixing; a_{12} describes the volume changes upon mixing monomers **1** and **2**; $\tilde{V}_{1,1}^\circ$ is the partial molar volume of polymer **1** in monomer **1**; $F_1 = 1 - F_2$ is the composition of monomer **1** in the copolymer; and F_{12} is the population of **1**–**2** chemical bonds in the copolymer. All the parameter values necessary to compute Γ° by using equations (2) and (3) were determined by measuring the densities of appropriate solutions[17] and are listed in *Table 1*.

Rates of polymerization and initiation

The rate of polymerization initiated by AIBN was determined as described previously[2,3]. Copolymers rich in ST and those rich in EA were precipitated into methanol and petroleum ether, respectively. The polymers were further purified by precipitation from a toluene solution into methanol or petroleum ether. Copolymer compositions were determined by combustion analysis for carbon.

The rate of initiation was determined by the inhibition method using HTMPO as an inhibitor. The experimental details have been described previously[2]. Some examples of the contraction *versus* time curves are given in *Figure 1*. When the ST content, f_1, in the feed was higher than about 0.3, the curve was linear after the onset of polymerization, giving well-defined inhibition times. However, for $f_1 < 0.3$, a retardation period was observed, in which case the inhibition time was determined by linearly extrapolating the final steady-rate part to the time axis.

Table 1 Values of the volumetric parameters for ST(**1**)/EA(**2**)/40°C system[a]

V_1	117.04	$\tilde{V}_{1,1}^\circ$	96.51
V_2	112.10	$\tilde{V}_{1,2}^\circ$	96.30
$10^3 \times a_{12}$	−1.60	$\tilde{V}_{2,2}^\circ$	86.40
ΔV_{12}	2.17	$\tilde{V}_{2,1}^\circ$	86.20

[a] See equations (2) and (3); V_i and ΔV_{12} are in ml mol^{-1}

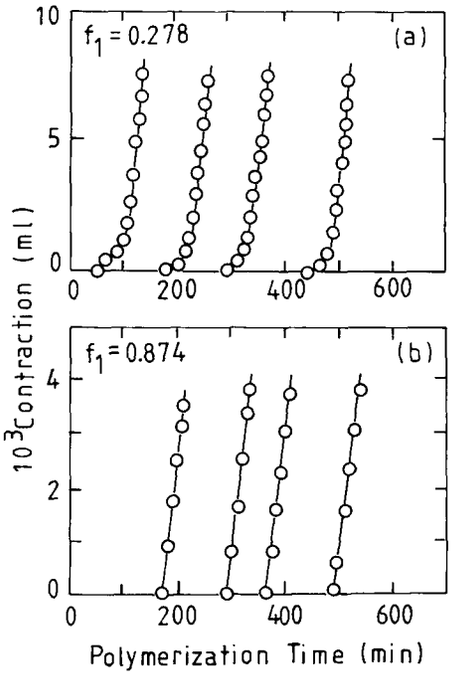

Figure 1 Plot of volume contraction *versus* polymerization time for ST/AIBN/40°C system: (a) $f_1 = 0.278$ and $10^2 \times$ [HTMPO]/[AIBN] = 0.375, 0.756, 1.000 and 1.630 (from left to right): (b) $f_1 = 0.874$ and $10^2 \times$ [HTMPO]/[AIBN] = 0.751, 1.372, 1.610 and 2.230 (from left to right)

Radical lifetime

The lifetime τ was determined by the r.s. method with ACN as a photosensitizer. The apparatus employed and experimental details were as described previously[2]. We previously reported that the steady-state polymerization rate, R_p, in the ST/MMA system decreased as conversion increased, even in a low-conversion region. Qualitatively the same dependence was observed in this system. Correction for this effect was made according to 'method 1' described previously[2]. Typical examples of the $\bar{R}_p/R_{pL}$ *versus* $\log t_L$ plot are presented in *Figure 2*, where $\bar{R}_p$ is the average rate of polymerization under intermittent illumination of light time t_L and dark time t_D ($t_D/t_L = 2$, in this case), and R_{pL} is the rate under steady illumination. An optimum value of τ was determined by a least-squares curve-fitting method. The solid line in each figure represents the theoretical curve[2] calculated with the optimum τ value.

RESULTS AND DISCUSSION

The rate of copolymerization, R_p, can be expressed formally by the same equation as for homopolymerization[2]:

$$R_p = \bar{\omega}[M]R_i^{1/2} \quad (4)$$

with

$$\bar{\omega} = \bar{k}_p/\bar{k}_t^{1/2} \quad (5)$$

$$R_i = 2f'k_d[I] \quad (6)$$

In these expressions, R_i is the rate of initiation, [M] is the total concentration of monomers and [I] is the concentration of initiator with a decomposition rate

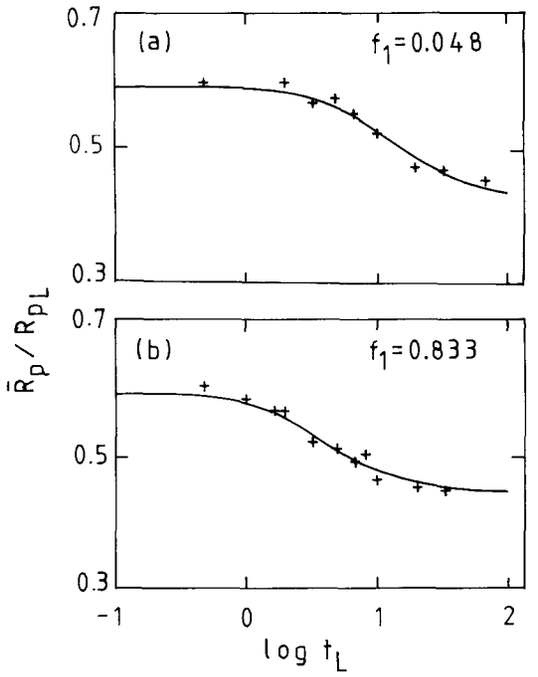

Figure 2 Plot of $\bar{R}_p/R_{pL}$ *versus* $\log t_L$ for ST/EA/ACN/40°C system: (a) $f_1 = 0.048$, $[ACN] = 2.449 \times 10^{-3}$ mol l^{-1}, and $R_{pD}/R_{pL} = 0.183$, where R_{pD} represents the polymerization rate in the dark (solid curve, for $\tau = 4.80$ s); (b) $f_1 = 0.833$, $[ACN] = 6.488 \times 10^{-3}$ mol l^{-1}, and $R_{pD}/R_{pL} = 0.170$ ($\tau = 1.48$ s)

constant k_d and efficiency f'. Insofar as $\bar{k}_p$ and $\bar{k}_t$ are constant, the radical lifetime can be determined by the same method as for homopolymerization, and the rate constant ratio $\bar{k}_p/\bar{k}_t$ is evaluated according to the familiar relation:

$$\tau R_p = (\bar{k}_p/\bar{k}_t)[M] \tag{7}$$

All copolymerization runs were carried out at low conversions (<4 wt%) so that composition drift with conversion may be neglected. Typical values of the number-average degree of polymerization of the recovered polymers were 1×10^3 or larger, apparently large enough for the long-chain approximation[2] to be applicable. *Table 2* summarizes the results of the steady-state runs initiated with AIBN.

Figure 3 shows the plot of the copolymer composition, F_1, against the feed-monomer composition, f_1. The data were fitted to the Mayo–Lewis equation[18]:

$$\frac{F_2}{F_1} = \frac{r_2 f_2^2 + f_1 f_2}{r_1 f_1^2 + f_1 f_2} \tag{8}$$

$$r_1 = k_{11}/k_{12}, \qquad r_2 = k_{22}/k_{21} \tag{9}$$

An optimum fit was obtained for $r_1 = 0.775$ and $r_2 = 0.165$ with a standard deviation of 1.2%. This deviation is about what would be expected from the analytical uncertainty (about $\pm 1.5\%$), which means that the composition of

Table 2 Summary of the steady-state copolymerization of ST and EA in the bulk at 40°C

Run	f_1[a]	[M][b] (mol l^{-1})	10^2[I][c] (mol l^{-1})	Y[d] (wt%)	t[e] (min)	F_1[f]	$10^4 R_p/[I]^{1/2}$ (mol$^{1/2}$ l$^{-1/2}$ s^{-1})
1	0.000	8.920	0.002				93.61[g,h]
2			0.007				
3			0.012				
4			0.135				
5			0.160				
6	0.031	8.908	2.803	3.72	83		3.957
7	0.047	8.902	3.914	3.83	92		3.104
8	0.057	8.898	1.989	1.98	90	0.226	2.299
9	0.103	8.878	2.144	2.18	123	0.310	1.779
10	0.161	8.858	1.928	1.90	133	0.382	1.504
11	0.194	8.849	1.949	1.79	124	0.414	1.509
12	0.263	8.819	1.887	1.43	106	0.465	1.430
13	0.341	8.788	2.073	1.53	113	0.527	1.363
14	0.381	8.773	1.950	1.18	92	0.531	1.336
15	0.503	8.729	2.771	1.08	82		1.146
16	0.558	8.706	0.930	1.17	146	0.650	1.202
17	0.606	8.689	3.460	1.37	92	0.676	1.154[h]
18			6.290	1.95	97		
19			9.000	1.35	56		
20			10.050	2.00	79		
21	0.696	8.655	1.022	1.15	147		1.115
22	0.764	8.630	1.303	1.11	142	0.753	0.986
23	0.825	8.608	1.076	1.07	149		0.993
24	0.858	8.596	2.035	0.81	82		0.993
25	0.906	8.578	1.313	1.03	140	0.867	0.922
26	1.000	8.544					0.943[i]

[a] Mole fraction of ST in feed
[b] Total monomer concentration
[c] AIBN concentration
[d] Conversion
[e] Polymerization time
[f] Mole fraction of ST in copolymer
[g] By dilatometry
[h] Average value
[i] From reference 2

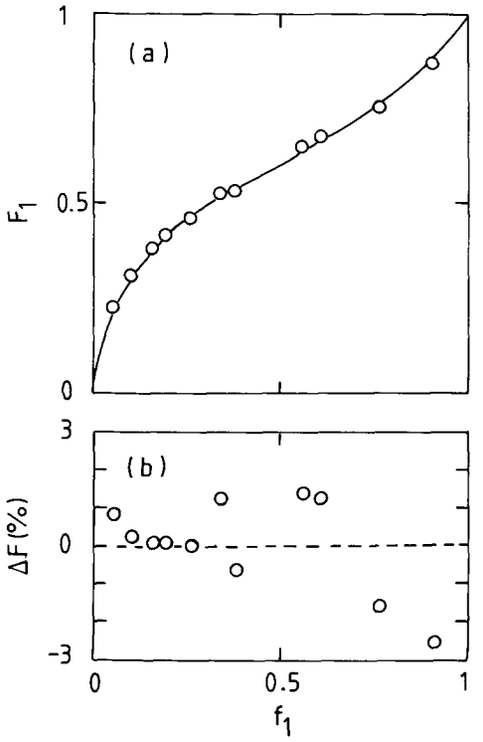

Figure 3 (a) Plot of F_1 *versus* f_1 for the ST/EA copolymer: the solid curve is the Mayo–Lewis equation[18] with $r_1=0.775$ and $r_2=0.165$; (b) plot of $\Delta F=F_{1,\text{obs.}}-F_{1,\text{calc.}}$ *versus* f_1

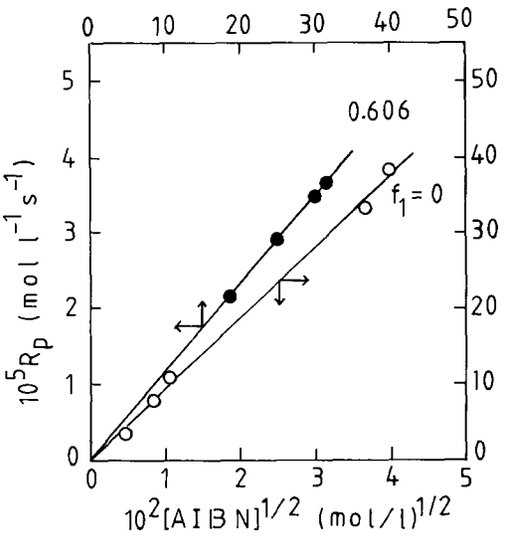

Figure 4 Plot of R_p *versus* [AIBN]$^{1/2}$ for ST/EA/AIBN/40°C system

this system conforms to the terminal model within the experimental error. The same conclusion has been reached for the ST/EA/50°C and ST/EA/benzene (BZ)/50°C systems[19].

In *Figure 4*, the rate of steady-state polymerization, R_p, is plotted against the square root of the initiator concentration, [AIBN]$^{1/2}$, for different values of f_1, showing proportionality to hold between these quantities, within experimental error.

In *Figure 5*, the inhibition time, t_i, is plotted against the inhibitor-to-initiator concentration ratio, [HTMPO]/[AIBN], for some values of f_1. In all cases examined, proportionality was found to hold between these quantities.

The values of $2f'k_d$ determined from the slopes of the plot are collected in *Table 3*. The dependence of $2f'k_d$ on f_1 may be approximated by the linear equation:

$$2f'k_d \times 10^6 = 0.537 + 0.209f_1 \quad (\text{in s}^{-1}) \qquad (10)$$

Similar results have been reported for the ST/EA/50°C and ST/EA/BZ/50°C systems[20]. From the values of $R_p/[I]^{1/2}$ given in *Table 2* along with equation (10), the parameter $\bar{k}_p/\bar{k}_t^{1/2}$ was evaluated, which is plotted against f_1 in *Figure 6*. The solid curve in the figure is the best-fit representation of the data, which will be used for the following analysis. Incidentally, if we analyse these data according to the Walling equation[21], we obtain values of the cross-termination factor ϕ ranging from about 20 to as large as about 800, depending on f_1. These ϕ values

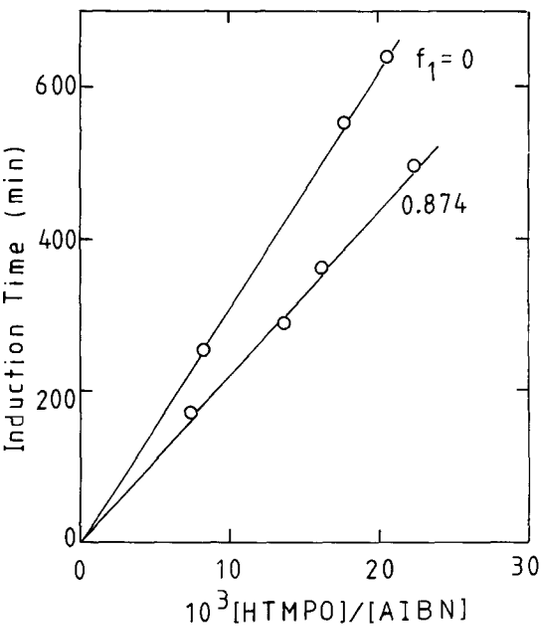

Figure 5 Plot of induction time *versus* inhibition-to-initiator concentration ratio for ST/EA/AIBN/HTMPO/40°C system

Table 3 Inhibition times of ST/EA/AIBN/HTMPO/40°C system

f_1	10^2[AIBN] (mol l^{-1})	10^4[HTMPO] (mol l^{-1})	t_i[a] (min)	$10^6(2f'k_d)$[b] (s^{-1})
0.000	0.158	0.130	253	0.537
	0.162	0.288	552	
	0.170	0.350	683	
0.278	2.126	0.760	100	0.551
	2.065	1.561	210	
	2.290	2.289	322	
	2.012	3.279	483	
0.478	0.136	0.048	105	0.628
	0.177	0.248	350	
0.721	2.378	1.682	170	0.660
	2.453	3.269	330	
	2.402	3.921	445	
	2.337	5.383	560	
0.874	0.173	0.130	170	0.760
	0.113	0.155	287	
	0.136	0.219	360	
	0.178	0.397	490	
1.000				0.746[c]

[a] Inhibition time
[b] Average value
[c] From reference 2

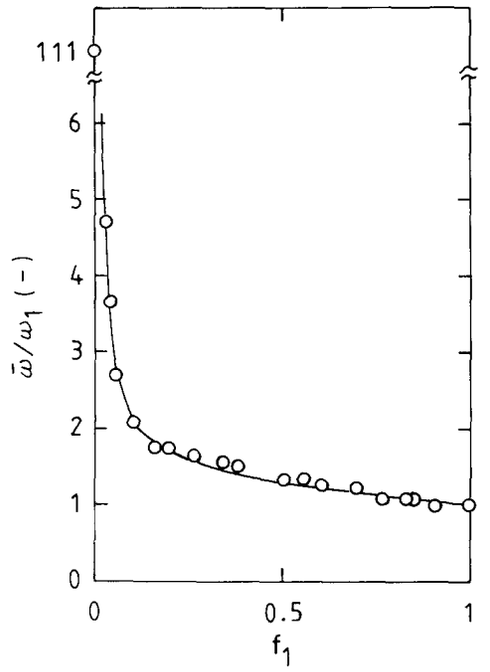

Figure 6 Plot of $\bar{\omega}/\omega_1$ *versus* f_1 for ST/EA/AIBN/40°C system. The solid curve is the best-fit representation of the experimental data

Table 4 Summary of the rotating-sector experiments for ST(**1**)/EA(**2**)/40°C system

f_1	10^3[ACN] (mol l^{-1})	$10^5 R_{pL}$[a] (mol l^{-1} s^{-1})	R_{pD}/R_{pL}	τ (s)
0.048	2.449	1.974	0.138	4.80
0.051	0.783	1.281	1.137	7.31
0.103	3.324	1.724	0.154	3.04
0.239	3.995	1.516	0.146	2.31
0.322	8.517	1.773	0.165	1.76
0.494	7.983	1.734	0.158	1.65
0.584	10.217	1.414	0.126	1.90
0.639	7.875	1.244	0.163	1.88
0.684	11.480	1.387	0.152	1.36
0.777	8.761	1.218	0.144	1.42
0.811	6.488	1.380	0.161	1.46
0.833	10.077	1.198	0.170	1.48

[a] An average value (see reference 2 for details)

Table 5 Values of $\bar{k}_p$ and $\bar{k}_t$ for ST(**1**)/EA(**2**)/40°C system[a]

f_1	$10^2\bar{k}_p/\bar{k}_t^{1/2}$[b] ($l^{1/2}$ mol$^{-1/2}$ s$^{-1/2}$)	$10^5\bar{k}_p/\bar{k}_t$	$\bar{k}_p$ (l mol^{-1} s^{-1})	$10^{-6}\bar{k}_t$ (l mol^{-1} s^{-1})
0.000	143	(43.2)[d]	(4700)	(11)
0.048	4.50	1.084	187	17
0.051	4.22	1.053	169	16
0.103	2.85	0.590	138	23
0.239	2.04	0.397	105	26
0.322	1.86	0.355	97	27
0.494	1.64	0.328	82	25
0.584	1.56	0.309	79	26
0.639	1.52	0.270	86	32
0.684	1.48	0.218	100	46
0.777	1.42	0.201	100	50
0.811	1.41	0.234	85	36
0.833	1.39	0.207	93	45
1.000[c]	1.29	0.140	120	86

[a] The viscosity η of this system is given by: $\eta = 0.609f_1 + 0.447f_2$ (in cP)
[b] Value read from the solid curve in *Figure 6*
[c] From reference 2
[d] From reference 22

are only 'apparent', since the Walling equation is based on the terminal propagation model (see below).

The radical lifetime was measured at 12 different values of f_1. Numerical results are listed in *Table 4*. These data were combined with the steady-state polymerization data to yield the individual values of $\bar{k}_p$ and $\bar{k}_t$ listed in *Table 5*. The attempt to measure τ at $f_1 = 0$ was unsuccessful because pure EA gelled too quickly to carry out a series of r.s. experiments. To our knowledge, there is only one reported value of k_p/k_t for EA at 40°C, which was obtained in toluene solution ([EA] = 1.84 mol l^{-1})[22]. This value ($k_p/k_t = 4.32 \times 10^{-4}$), combined with our data, gives $k_p = 4700$ and $k_t = 11 \times 10^6$ l mol^{-1} s^{-1}. This k_t value does not appear too unreasonable with regard to those observed here at low ST compositions (cf. *Table 5* and *Figure 8*). Using the p.l.p. technique[23], Davis *et al.*[8] suggested that k_p values of MA and BA at 40°C are no smaller than 3400 and 2800, respectively. In this regard, the above-noted k_p value for EA may also be reasonable, or at least correct in order of magnitude. Thus we will tentatively adopt these values of k_p and k_t for the following analyses.

Propagation process

We now examine the $\bar{k}_p$ data. In *Figure 7*, the observed values of $\bar{k}_p$ are compared with those calculated with the terminal model equation[2]:

$$\bar{k}_p = \frac{r_1 f_1^2 + 2f_1 f_2 + r_2 f_2^2}{(r_1 f_1/k_{11}) + (r_2 f_2/k_{22})} \tag{11}$$

with $r_1 = 0.775$, $r_2 = 0.165$, $k_{11} = 120$ and $k_{22} = 4700$. The disagreement between the model and experiment is evident. As mentioned above, the value of k_{22} involves considerable uncertainty. However, it can be easily

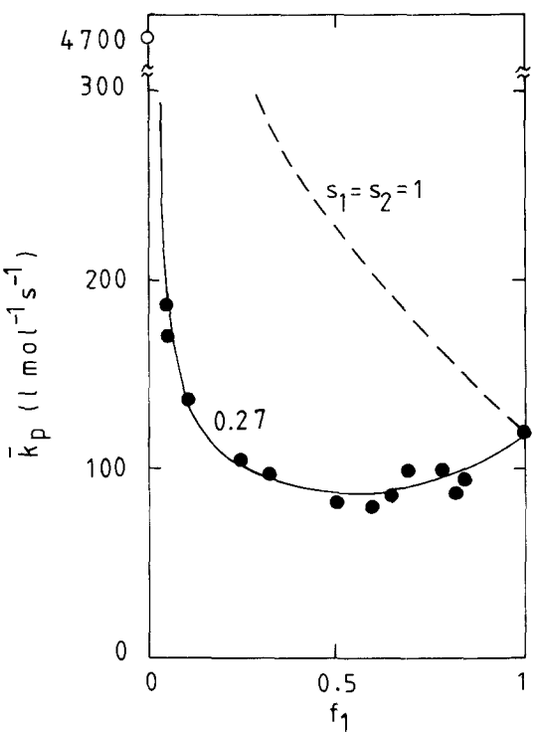

Figure 7 Plot of $\bar{k}_p$ *versus* f_1 for the ST/EA/40°C system: ●, measured values; —, calculated with the penultimate model, with $r_1 = 0.775$, $r_2 = 0.165$, $k_{111} = 1201$ mol^{-1} s^{-1}, $k_{222} = 4700$ l mol^{-1} s^{-1} and $s_1 = s_2 = 0.27$; – – –, the terminal model ($s_1 = s_2 = 1$)

confirmed that the calculated result is quite insensitive to k_{22}, insofar as $k_{22} > 500$, which is definitely the case. We thus conclude that the ST/EA system does not conform to the terminal model.

Qualitatively the same conclusions have been obtained for the ST/MA and ST/BA systems by Davis *et al.*[8]. Quantitatively, however, there are considerable differences between the results of Davis *et al.* and our results. As *Figure 7* shows, the $\bar{k}_p$ curve of the ST/EA system (40°C) has a shallow minimum at an intermediate composition. We have observed a very similar curve for the *p*-chlorostyrene (*p*CS)/MA system[3]. On the other hand, the $\bar{k}_p$ curves for the ST/MA and ST/BA systems at 50°C have no such minimum and are closer to the terminal-model curves than the ST/EA curve observed here. At a lower temperature (25°C), the ST/MA and ST/BA curves come even closer to the terminal-model curves[8]. In view of the similarity of the studied systems, these quantitative differences appear to be inconsistent. The reason is unclear.

As in the case of the ST/MMA systems[2,4], the failure of the terminal model in the ST/EA system may be ascribed to a p.u.e. Since the composition curve conforms to the terminal model (see below), we may assume r_1 and r_2 to be constant, independent of composition. Then the terminal model $\bar{k}_p$ is given by equation (11) with k_{11} and k_{22} replaced by $\bar{k}_{11}$ and $\bar{k}_{22}$, respectively[2]:

$$\bar{k}_{11} = k_{111}(r_1 f_1 + f_2)/(r_1 f_1 + s_1^{-1} f_2) \quad (12)$$

$$\bar{k}_{22} = k_{222}(r_2 f_2 + f_1)/(r_2 f_2 + s_2^{-1} f_1) \quad (13)$$

For s_1 and s_2, see the definitions following equation (1). In this system, r_2/k_{222} is smaller than r_1/k_{111} by a factor of about 180, and therefore it is virtually impossible to determine s_2 with meaningful accuracy (cf. equation (11)). For this reason, we simply assume that $s_1 = s_2$. The solid curve in *Figure 7* shows the result of optimization, giving $s_1 = 0.27$. It can be confirmed that this s_1 value is insensitive to the choice of the k_{222} value if $k_{222} \geqslant 500$. Alternatively, if one assumes that $s_2 = 1$, virtually the same result is obtained. Thus the estimate of $s_1 = 0.27$ is reliable enough, while s_2 remains unknown. (It is noted that the results of Davis *et al.*[8] for the two systems mentioned show that s_1 does not differ significantly from unity, while s_2 is very small. In this regard, their results are qualitatively different from ours.)

Equation (1) predicts that, for this system, $s_1 s_2 \approx r_1 r_2 = 0.13$, or under the assumption of $s_1 = s_2$, that $s_1 \approx 0.36$. This value is similar in order of magnitude to the experimental value. This result would reinforce the stabilization energy model[11,12].

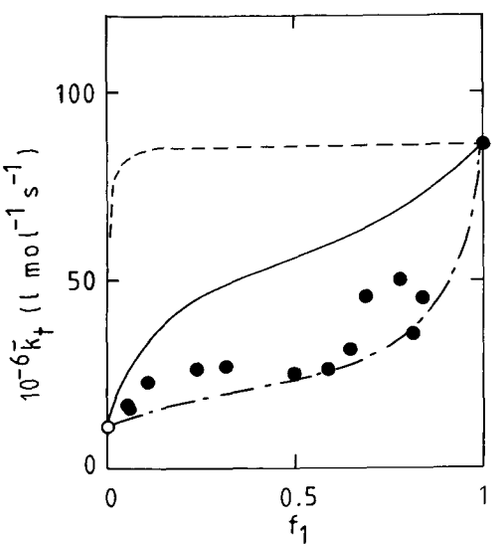

Figure 8 Plot of $\bar{k}_t$ *versus* f_1 for the ST/EA/40°C system: – – –, the chemical model of Walling with $\phi = 0$; ——, the diffusion model of North; —·—, the diffusion model given by equation (15)

Termination process

In *Figure 8*, the observed values of $\bar{k}_t$ are shown as a function of f_1. It is seen that all of the copolymerization data points fall between k_{t1} and k_{t2}, indicating that the termination step is controlled by 'diffusion'. If one estimates $\bar{k}_t$ using the experimental value of $\bar{k}_p/\bar{k}_t^{1/2}$, with $\bar{k}_p$ assumed to be given by the terminal model, one obtains extremely large values of $\bar{k}_t$, especially at small values of f_1. For example, at $f_1 = 0.1$ the estimated value is more than 10 times larger than the correct (observed) one. In fact, the chemically controlled model[21] fails to describe the experiment for any positive value of ϕ, as indicated by the broken curve ($\phi = 0$) in the figure.

The solid curve in *Figure 8* represents the North model[24]:

$$\bar{k}_t = F_1 k_{t1} + F_2 k_{t2} \quad (14)$$

As the figure shows, this model does not describe the experiment very accurately.

If diffusion is rate controlling, it may be physically more reasonable to consider that $\bar{k}_t$ is inversely proportional to the friction coefficient ζ (ref. 25). With other conditions assumed to be the same, the averaging of ζ with respect to copolymer composition gives the following no-parameter model:

$$\bar{k}_t^{-1} = F_1 k_{t1}^{-1} + F_2 k_{t2}^{-1} \quad (15)$$

This model is conceptually analogous to that of Ito and O'Driscoll[1], which involves a higher-order averaging of ζ. Despite its simplicity, equation (15) is numerically close to the Ito–O'Driscoll model.

The dot–dash line in *Figure 8* represents equation (15). As far as this system is concerned, equation (15) describes the experiment better than equation (14). However, this does not necessarily imply a general validity of equation (15). The termination reaction in copolymerization should be a complicated process in which the diffusional motions of the whole chain or the chain end (or both) would take part. A better understanding of the termination and propagation processes in radical copolymerization requires more high-quality experiments as well as theoretical considerations.

CONCLUSION

A fairly strong penultimate-unit effect was observed for the terminal ST radical ($s_1 = 0.27$), the magnitude of which can be interpreted by the stabilization energy model. The termination process of the ST/EA system is better described by the new no-parameter model based on the notion of diffusion-controlled termination, rather than by the 'ideal' diffusion model of North.

REFERENCES

1 Ito, K. and O'Driscoll, K. F. *J. Polym. Sci., Polym. Chem. Edn* 1979, **17**, 3913

2 Fukuda, T., Ma, Y.-D. and Inagaki, H. *Macromolecules* 1985, **18**, 17
3 Ma, Y.-D., Fukuda, T. and Inagaki, H. *Macromolecules* 1985, **18**, 26
4 Fukuda, T., Kubo, K., Ma, Y.-D. and Inagaki, H. *Polym. J.* 1987, **19**, 523
5 Davis, T. P., O'Driscoll, K. F., Piton, M. C. and Winnik, M. A. *J. Polym. Sci., Polym. Lett. Edn* 1989, **27**, 181
6 Davis, T. P., O'Driscoll, K. F., Piton, M. C. and Winnik, M. A. *Macromolecules* 1990, **23**, 2113
7 Olaj, O. F., Schnöll-Bitai, I. and Kremminger, P. *Eur. Polym. J.* 1989, **25**, 535
8 Davis, T. P., O'Driscoll, K. F., Piton, M. C. and Winnik, M. A. *Polym. Int.* 1991, **24**, 65
9 Piton, M. C., Winnik, M. A., Davis, T. P. and O'Driscoll, K. F. *J. Polym. Sci., Polym. Chem. Edn* 1990, **28**, 2097
10 Sato, T., Takahashi, K., Tanaka, H., Ohta, T. and Kato, K. *Macromolecules* 1991, **24**, 2330
11 Fukuda, T., Ma, Y.-D. and Inagaki, H. *Makromol. Chem., Rapid Commun.* 1987, **8**, 495
12 Fukuda, T., Kubo, K., Ma, Y.-D. and Inagaki, H. *Macromolecules* 1991, **24**, 370
13 Fukuda, T., Kubo, K. and Ma, Y.-D. *Prog. Polym. Sci.* 1992, **17**, 875
14 Kim, P.-S. MSc dissertation, Dankook University, Korea, 1987
15 Fukuda, T., Ma, Y.-D., Nagata, M. and Inagaki, H. *Polym. J.* 1982, **14**, 729
16 Ma, Y.-D., Fukuda, T. and Inagaki, H. *Polym. J.* 1983, **15**, 673
17 Ma, Y.-D. and Han, C.-Y. *Dankook Univ. Fac. Res. Papers*, 1986, **20**, 261
18 Mayo, F. R. and Lewis, A. N. *J. Am. Chem. Soc.* 1944, **66**, 1954
19 Fehérvári, A., Földes-Berezsnich, T. and Tüdös, F. *J. Makromol. Sci. Chem.* 1982, **A18**, 337
20 Fehérvári, A., Földes-Berezsnich, T. and Tüdös, F. *J. Makromol. Sci. Chem.* 1981, **A16**, 993
21 Walling, C. *J. Am. Chem. Soc.* 1949, **71**, 1930
22 Rätzsch, M. and Zschach, J. *Plaste Kautschuk* 1974, **21**, 345
23 Olaj, O. F., Bitai, I. and Hinklemann, F. *Makromol. Chem.* 1987, **188**, 1689
24 Atherton, J. A. and North, A. M. *Trans. Faraday Soc.* 1962, **58**, 2049
25 Mahabadi, H. K. and O'Driscoll, K. F. *J. Polym. Sci., Polym. Chem. Edn* 1977, **15**, 283